PNAS PNAS PNAS PNAS

# Supporting Information

Caron et al. 10.1073/pnas.1301342110

## SI Materials and Methods

**Plasmid Constructs.** The huntingtin exon1 fragments with various glutamine lengths were generated from cDNA using forward primer GATCTCCGGAATGGCGACCCTG with a BSP E1 restriction site and reverse primer GATCGGTACCGGGTCG-GTGCAGCGGCTC with an ACC65I site. Huntingtin exon1 M8P, S13, and S16 mutants were generated from larger huntingtin 1-586 fragments described previously (1), using forward and reverse primers described above. The 1-117 fragments were generated using the same forward primer as for the exon1 constructs and the reverse primer GATCGGTACCGACAGACT-GTGCCAC with an ACC65I restriction site. The 1-171 fragments were also generated using the same forward primer as for the exon1 constructs and the reverse primer GATCGGTACCCCTC-GAGCTGTAACCTTGG with an ACC65I restriction site. The 1-220 fragments were also generated using the same forward primer as for the exon1 constructs and the reverse primer GATCGGTACCCTTGCTTGTTCGAGTCAG with an ACC65I restriction site. The 1-465 fragments were also generated using the same forward primer as for the exon1 constructs and the reverse primer GATCGGTACCGCTGCTGACATCCGATCT with an ACC65I restriction site. All insert PCR products were cloned into a modified mCer-C1plasmid with an eYFP insert cloned into BamHI and XbaI sites at the opposing end of the multiple cloning site.

**Immunofluorescence.** ST*Hdh*$^{Q7/Q7}$ cells were seeded to ~80% confluency before fixation and permeabilization with ice-cold methanol at −20 °C for 12 min. Cells were then washed 2 times with PBS and blocked 2 times with 2% (vol/vol) FBS in PBS. Primary antibodies for PACSIN1 (A-3, catalog no. sc-166756, 1:50–100), N17 (generated to epitope MKAFESLKSFQC, 1:250), and phospho-N17 S13 and S16 (generated to epitope MKA-FESpLKSpFQC, 1:250) were then added to cells in a solution with 0.0002% Tween 20 (Sigma, catalog no. P9416), 2% (vol/vol) FBS in PBS overnight and subsequently washed 2 times with blocker solution. Secondary antibodies raised against rabbit (Alexa Fluor 488 donkey anti-rabbit, catalog no. A21206, 1:500) or mouse (Alexa Fluor 594 goat anti-mouse, catalog no. A11032, 1:500) were then added to cells in antibody solution for 45 min and subsequently washed 2 times with PBS before imaging.

**Immunofluorescence for Antibody-Based FLIM.** Cells were seeded to 80% confluency before fixation for 30 min using 4% (wt/vol) paraformaldehyde. Cells were washed 3 times with PBS before being permeabilized with 0.5% (vol/vol) Triton X-100, 2% (vol/vol) FBS in PBS for 15 min. Cells were then washed 2 times with PBS and blocked 2 times with 2% FBS in PBS. Primary conjugated antibodies were then added to cells at optimized concentrations in a solution with 0.0002% Tween 20 (Sigma, catalog no. P9416), 2% (vol/vol) FBS in PBS for ~16 h each and subsequently washed 2 times with PBS.

**Microscopy.** Widefield fluorescence images were captured on a Nikon TE200 epifluorescence inverted microscope equipped with a 63× oil immersion NA1.4 plan apochromat objective using a Hamamatsu Orca ER camera (Hamamatsu Photonics).

1. Atwal RS, et al. (2011) Kinase inhibitors modulate huntingtin cell localization and toxicity. *Nat Chem Biol* 7(7):453–460.

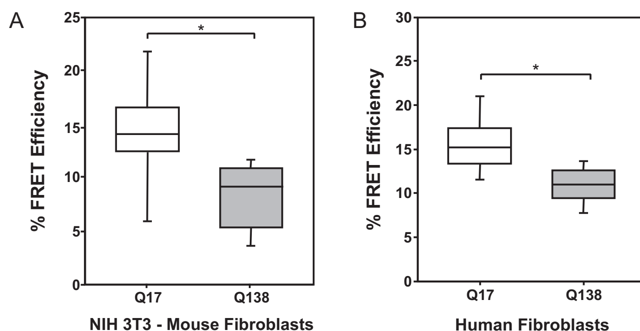


**Fig. S1.** Huntingtin FRET sensor in fibroblasts. Quantification of huntingtin exon1 FRET sensor with either wild-type (Q17) or mutant (Q138) polyglutamine lengths in (*A*) NIH 3T3 mouse fibroblasts or (*B*) human fibroblasts. *$P < 0.001$. $n = 30$, 3 replicate trials and $n = 70$, 3 replicate trials, respectively. (Scale bars: 10 μm.)

**Fig. S2.** Measuring the conformation of wild-type and mutant polyglutamine tracts in the context of longer huntingtin fragments. Quantification of various huntingtin FRET sensors in different fragment length contexts with either wild-type or mutant polyglutamine lengths. FRET efficiency drops when the acceptor is placed at 171 or further downstream, with no notable differences between wild-type and expanded polyglutamine lengths. *$P < 0.001$, NS = not statistically significant. $n = 15$, 3 replicate trials. (Scale bars: 10 μm.)

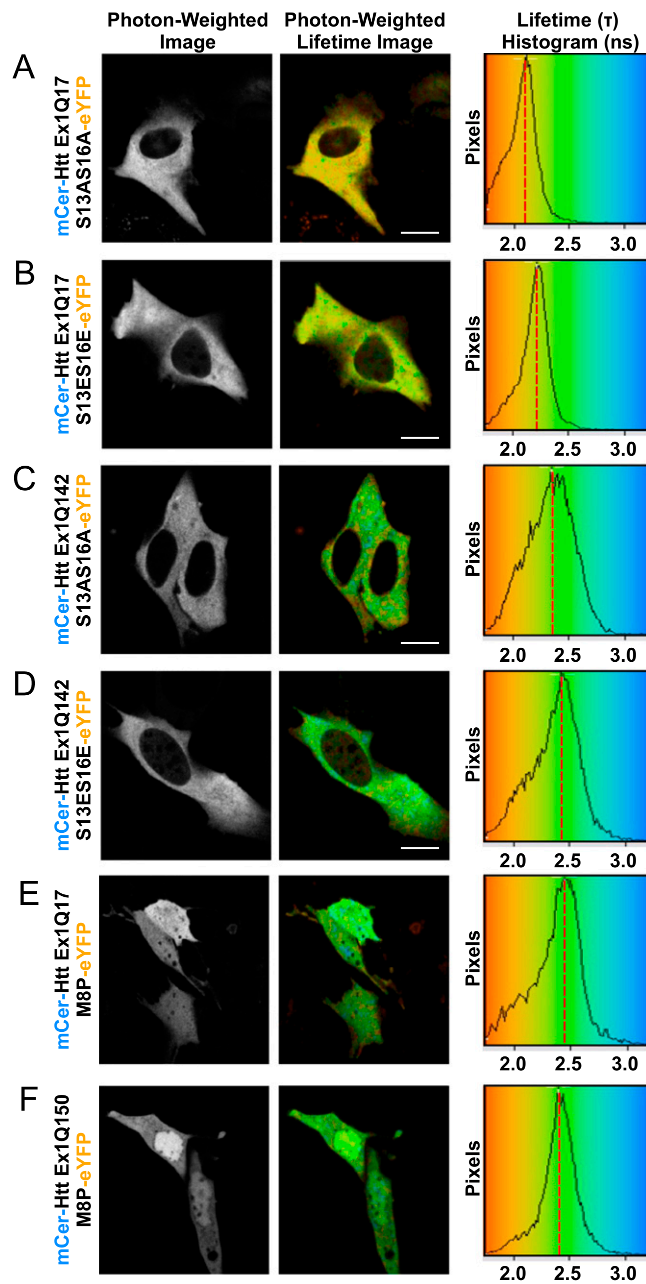


**Fig. S3.** N17 phosphomimicry mutants can affect the conformation of huntingtin exon1. (*A*–*D*) Sample live-cell FLIM images of mCerulean-HttEx1 Q17 or Q142-eYFP constructs with serine 13 and 16 point mutations expressed in ST*Hdh*$^{Q7/Q7}$ cells. Sample FLIM images of (*E*) mCer-HttEx1 Q17-YFP or (*F*) mCer-HttEx1 Q150-eYFP with the M8P loss-of-structure mutation in N17 (note nuclear localization).

**Fig. S4.** Coimmunoprecipitation and siRNA of PACSIN1. (*A*) Representative coimmunoprecipitation of endogenous PACSIN1 using a N17-eYFP fusion in ST*Hdh*$^{Q7/Q7}$. (Scale bars: 10 μm.) (*B*) Western blot showing levels of PACSIN1 knock-down following treatment of ST*Hdh*$^{Q7/Q7}$ cells with three siRNAs targeted toward mouse PACSIN1. Actin was used to control for equal loading. (*C*) Quantification on Western blots of PACSIN1 knockdown following 48 h treatments with PACSIN1 siRNA. (*D*) Immunofluorescence for PACSIN1 following treatment of cells with siRNA to PACSIN1. Images were taken at 80 ms exposure. (Scale bars: 10 μm.) (*E*) FRET efficiency for either venus-HttEx1 Q17-mCherry or venus-HttEx1 Q138-mCherry following treatment with a control siRNA or against endogenous PACSIN1. $^{*}P < 0.001$. $n = 15$, 3 replicate trials.

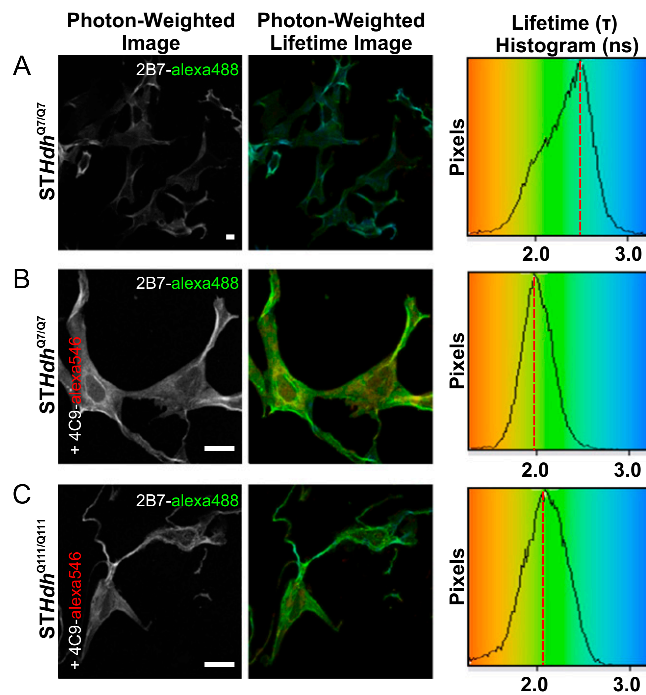


**Fig. S5.** FLIM-FRET of endogenous huntingtin using monoclonal antibodies. (*A*) FLIM image of 2B7-alexa488 conjugate in fixed STHdhQ7/Q7 cells. FLIM image of 2B7-alexa488 and 4C9-alexa555 conjugates in fixed (*B*) STHdhQ7/Q7 or (*C*) STHdhQ111/Q111 cells.